Active-Site Conformational Changes Associated with Hydride Transfer in Proton-Translocating Transhydrogenase[†,‡]

Owen C. Mather, Avtar Singh, Gijs I. van Boxel, Scott A. White,* and J. Baz Jackson*

School of Biosciences, University of Birmingham, Edgbaston, Birmingham B15 2TT, U.K.

Received February 3, 2004; Revised Manuscript Received April 29, 2004

ABSTRACT: Transhydrogenase couples the redox (hydride-transfer) reaction between NAD(H) and NADP(H) to proton translocation across a membrane. The redox reaction is catalyzed at the interface between two components (dI and dIII) which protrude from the membrane. A complex formed from recombinant dI and dIII (the dI_2dIII_1 complex) from *Rhodospirillum rubrum* transhydrogenase catalyzes fast single-turnover hydride transfer between bound nucleotides. In this report we describe three new crystal structures of the dI_2dIII_1 complex in different nucleotide-bound forms. The structures reveal an asymmetry in nucleotide binding that complements results from solution studies and supports the notion that intact transhydrogenase functions by an alternating site mechanism. In one structure, the redox site is occupied by NADH (on dI) and NADPH (on dIII). The dihydronicotinamide rings take up positions which may approximate to the ground state for hydride transfer: the redox-active $C4_N$ atoms are separated by only 3.6 Å, and the perceived reaction stereochemistry matches that observed experimentally. The NADH conformation is different in the two dI polypeptides of this form of the dI_2dIII_1 complex. Comparisons between a number of X-ray structures show that a conformational change in the NADH is driven by relative movement of the two domains which comprise dI. It is suggested that an equivalent conformational change in the intact enzyme is important in gating the hydride-transfer reaction. The observed nucleotide conformational change in the dI_2dIII_1 complex is accompanied by rearrangements in the orientation of local amino acid side chains which may be responsible for sealing the site from the solvent and polarizing hydride transfer.

There are many important proteins that couple a chemical transformation step to the translocation of solutes/ions across membranes. They include the ABC transporters, the phosphoenolpyruvate-dependent phosphotransferases, and the P-type, F-type, and V-type ATPases. Recent structure determinations indicate that the conformational changes responsible for coupling in some of these proteins are large and involve subunit rearrangements that establish new interfaces between domains (*1*−*3*). Currently, a considerable research effort is to define the character of these rearrangements and to discover the mechanisms by which the conformational changes are (reversibly) linked to chemical transformation and to solute/ion translocation. It is likely that underlying principles are similar in different proteins. Differential expression of ligand-binding energies at appropriate points in the reaction cycle will provide driving forces for protein motions, and gating devices to switch ligand access and a means to transmit information across the protein to synchronize key steps are essential. The proton pump, transhydrogenase, offers an opportunity to investigate one mechanism in which conformational changes for transmission to ion translocation sites are propagated by chemical transformation. A subcomplex of transhydrogenase (the dI_2dIII_1 complex), which catalyzes this primary event, is amenable to structure investigations and to studies on the reaction kinetics and protein dynamics. In this report we identify, using X-ray crystallography, conformational changes that appear to be associated with the reaction chemistry.

Transhydrogenase, which is found in the inner membranes of animal mitochondria and the cytoplasmic membranes of bacteria, couples the redox (hydride-transfer) reaction between NAD(H) and NADP(H) to proton translocation (Figure 1). For reviews, see refs *4*−*6*. The functions of transhydrogenase are tissue- and species-specific (*7*). Under many physiological conditions, the reaction is driven "forward" (toward $NADP^+$ reduction and NADH oxidation) by the proton electrochemical gradient (Δp) generated by the respiratory (sometimes photosynthetic) electron-transport chain. Then, either the product NADPH is used in biosynthesis and in glutathione reduction (needed to minimize structural damage caused by free radicals) or, in combination with the NAD- and NADP-dependent isocitrate dehydrogenases, the enzyme "microcycles" the nucleotides and thus ties the fine regulation of the TCA cycle to the value of Δp (*8*). In some anaerobic organisms, a "reverse" transhydrogenase reaction augments Δp formation to assist in the generation of ATP (*9*).

[†] Supported by grants from the Biotechnology and Biological Sciences Research Council and the Wellcome Trust.

[‡] Protein Data Bank codes for transhydrogenase structures are given throughout the text. Newly deposited PDB files are 1U28, 1U2D, 1U2G, and 1U31. The NAD(P)(H) atoms are numbered according to the IUPAC−IUB system.

* Corresponding authors. Telephone: +44 (0) 121 414 5423. Fax: +44 (0) 121 414 5925. E-mail: j.b.jackson@bham.ac.uk and s.a.white@bham.ac.uk.

10.1021/bi0497594 CCC: $27.50 © 2004 American Chemical Society
Published on Web 08/07/2004

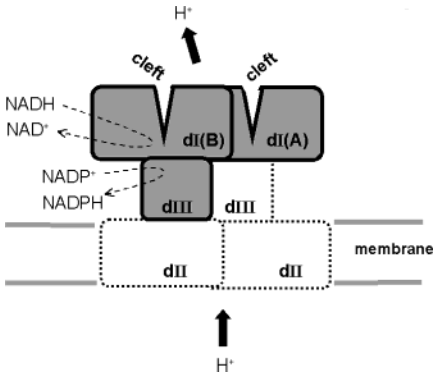

FIGURE 1: Domain structure of transhydrogenase. The gray-shaded regions represent the dI_2dIII_1 complex. The two dI polypeptides each comprise two domains, dI.1 and dI.2, which are separated by a deep cleft. The dIII component comprises a single domain. The dI polypeptide in the complex whose cleft is not associated with dIII is designated dI(A), and the dI polypeptide which is closely associated with dIII is designated dI(B). The intact, membrane-located enzyme is a dimer of two dI-dII-dIII monomers: the predicted organization of components that are absent in the dI_2dIII_1 complex is shown by the dotted lines. The dII component is thought to have 12, 13, or 14 transmembrane helices, depending on species (*64*, *65*). The dI and dIII components protrude from the membrane on the cytoplasmic side in bacteria and on the matrix side in mitochondria. The dashed arrows depict forward transhydrogenation and the thick solid arrows, the corresponding direction of proton translocation.

Transhydrogenase is a moderately sized protein comprising three components. The dI component (~400 amino acid residues), which binds NAD^+/NADH, and the dIII component (~200 residues), which binds $NADP^+$/NADPH, protrude from the membrane, and dII (~400 residues) spans the membrane (Figure 1). The intact protein is a "dimer" of two dI-dII-dIII[1] "monomers", although there is variability in the polypeptide composition among species. High-resolution structures of the membrane-peripheral components in various nucleotide-bound forms from both animal and bacterial sources have recently been published (*10*−*19*). A minimal mechanism for energy coupling was developed from observations on the enzyme's reaction kinetics and nucleotide-binding affinities (*5*): the monomers of transhydrogenase operating in the forward direction, for example, are driven from the "open" to the "occluded" conformational states, and then back to the open state, by protonation/deprotonation associated with the translocation reactions (*20*−*22*). Product nucleotides are released and fresh substrate nucleotides bind only in the open state, and hydride transfer takes place only in the occluded state. The conformational changes associated with on and off switching of hydride transfer are crucial for tight coupling between the redox reaction and proton translocation. From an examination of structures of the nucleotide-binding components of transhydrogenase, we proposed that relative movements of the 1,4-dihydronicotinamide ring of NADH and the nicotinamide ring of $NADP^+$ between "distal" and "proximal" positions are an important feature of the switch (*15*, *17*, *18*). Although the switching of chemical specificity is a feature of all coupled translocators (*23*), there is a particularly acute problem in transhydrogenase since the dihydronicotinamide and nicotinamide rings are highly reactive: to prevent a noncoupled redox reaction, they must be kept apart on the enzyme until the appropriate step in the reaction is reached. Here we present evidence for our proposals and further information on the character of the conformational changes in the nucleotides and protein.

In the absence of dII, simple mixtures of recombinant dI and dIII from *Rhodospirillum rubrum* transhydrogenase form a stable dI_2dIII_1 complex (*24*) which catalyzes very rapid single turnovers of hydride transfer between bound nucleotides (*25*, *26*). A second dIII component will bind to produce a dI_2dIII_2 complex but only with extremely low affinity (*27*). The X-ray structure of the dI_2dIII_1 complex was solved to 2.5 Å resolution (*15*). Its asymmetry, taken together with earlier experiments using chemical modification reagents that suggested half-of-the-sites reactivity (*28*, *29*), indicates an alternating-site mechanism for the intact enzyme: as one dI-dII-dIII monomer enters the open state to permit product release and substrate binding, the other enters the occluded state to permit hydride transfer. The dI(B)-dIII polypeptides of the dI_2dIII_1 complex (see Figure 1 for nomenclature) adopt a conformation which resembles that of the occluded state, and the dI(A) polypeptide is essentially in its open state (*15*).

Probably because of asymmetries in the nucleotide-binding properties of the dI_2dIII_1 complex, the X-ray data obtained on crystals grown in the presence of 5 mM NAD^+ and 5 mM $NADP^+$ (*15*) revealed good electron density for the $NADP^+$ in dIII and for the NAD^+ in dI(A) but only very weak density in the NAD(H)-binding site of dI(B). To visualize the hydride-transfer reaction, an NADH was modeled into the dI(B) site in the conformation of the NAD^+ in dI(A). The pyrophosphate and ribose−phosphate bonds of the modeled NADH were then rotated to bring the redox-active $C4_N$-H atom of its dihydronicotinamide ring into hydride-transfer distance with $C4_N$ of the $NADP^+$. We suggested that these modeled rotations reflect real events during the interconversion of the open and occluded states in the intact enzyme: the rotations are central to the on/off switch for hydride transfer. In the present work we have performed experiments in which we attempted to fill all of the nucleotide-binding sites in the dI_2dIII_1 complex and thus obtain a better view of the hydride-transfer reaction and associated conformational changes. The results provide strong support for the earlier modeling studies and begin to indicate how *local* changes at the active site might propagate the *interdomain* conformational changes that are involved in coupling to proton translocation.

EXPERIMENTAL PROCEDURES

The dI and dIII proteins of *R. rubrum* transhydrogenase and the dIII protein of human transhydrogenase were prepared as described (*30*−*32*). *R. rubrum* dI is a discrete polypeptide in the intact enzyme. In both *R. rubrum* and human transhydrogenases, the dIII components are on the same polypeptide chain as dII. Stop codons were therefore introduced by site-directed mutagenesis to isolate the DNA encoding just the dIII components. All three proteins were expressed to high yields in induced, appropriately engineered cells of *Escherichia coli* and were purified by column chromatography. The quality of the proteins was routinely checked by SDS−PAGE and by measuring rates of cyclic

[1] Abbreviations: asu, aymmetric unit; ADPR, adenosine 5′-diphosphoribose; dI, the NAD(H)-binding component of transhydrogenase; dII, the membrane-spanning component; dIII, the NADP(H)-binding component.

Table 1: Data Collection and Refinement Statistics[a]

data set	1U28	1U2D	1U2G	1U31
cell dimensions (Å)	71.7 × 73.9 × 204.2	72.3 × 74.6 × 204.2	72.4 × 73.8 × 205.0	57.8 × 57.8 × 250.9
no. of observations	214162 (19270)	154069 (21818)	231170 (16709)	60151 (3329)
no. of unique observations	47505 (5633)	22872 (3246)	55412 (7070)	19463 (1982)
completeness (%)	96.7 (80.8)	100 (100)	97.8 (87.0)	82.4 (66.5)
redundancy	4.5 (3.4)	6.7 (6.7)	4.2 (2.4)	3.2 (1.7)
$I/\sigma I$	11.6 (2.3)	20.3 (3.6)	17.0 (2.1)	10.6 (10.4)
R_{sym} (%)[b]	7.7 (41.3)	10.7 (56.5)	4.6 (42.5)	4.9 (5.6)
resolution range (Å)	49−2.3 (2.42−2.3)	50−3.0 (3.16−3)	46−2.2 (2.32−2.2)	63−2.3 (2.46−2.3)
R factor[c] (%)	22.8 (27.0)	21.0 (34.0)	23.2 (35.0)	22.9 (28.8)
R free[d] (%)	29.2 (40.0)	26.7 (42.0)	25.9 (39.0)	28.1 (31.9)
RMSD bond angles[e] (deg)	1.15	1.23	1.18	1.61
RMSD bond lengths[e] (Å)	0.008	0.008	0.007	0.007

[a] Values in parentheses indicate data in the highest resolution shell. [b] $R_{sym} = \sum_n|\langle I\rangle - I_n|/\sum\langle I\rangle$, where I_n is the intensity of the *n*th reflection and $\langle I\rangle$ is the average intensity of symmetry-related reflections. [c] *R* factor $= \sum_{hkl}||F_o| - |F_c||/|F_o|$. [d] *R* free = *R* factor based upon 5% of the data withheld from the refinement process. [e] RMSD bond lengths and angles are the root mean square deviations from ideal bonds and angles, respectively.

transhydrogenation in dI_2dIII_1 complexes. The proteins were stored in 25% glycerol at −20 °C before use. The numbering system for the amino acid sequences is as described in ref *15*. The NAD(P)(H) atoms are numbered according to the IUPAC−IUB system as described (*33*). Thus, $C4_N$ is the *c*arbon atom at position *4* of the *n*icotinamide ring.

Crystallization of *R. rubrum* dI_2dIII_1 complexes was carried out at the nucleotide concentrations described in Table 2 and after optimizing the conditions outlined in ref *15*. In all three cases, the buffer was 100 mM 2-morpholinoethanesulfonic acid, pH 6.5, containing 10% glycerol. For the NADH−NADPH crystals, 38−60 mM ammonium sulfate and 21−23% 8K poly(ethylene glycol) were optimal, and for both the NAD^+−$NADP^+$ crystals and the ADPR−NADPH crystals, 24−74 mM ammonium sulfate and 18−22% 8K poly(ethylene glycol) were optimal. Crystals of sufficient size for data collection (typically 0.1 × 0.1 × 0.07 mm for all three liganded forms) were obtained without seeding. They were formed within 1 week of setting up the drops. Crystals were removed from the mother liquor, soaked in a similar solution (but one containing fresh nucleotides and supplemented with 18% glycerol), and then plunged into liquid nitrogen for storage before mounting in the X-ray beam at the European Synchrotron Radiation Facility at Grenoble. Data sets were collected for different nucleotide combinations as shown in Tables 1 and 2. The data were integrated and scaled using the programs MOSFLM (*34*) and SCALA (*35*). Each of the structures was refined independently in REFMAC (*36*) using 1HZZ (see Table 1), with its nucleotides and waters removed, as a starting model (*15*).

Isolated human dIII in its NADPH form was crystallized essentially as described for the oxidized form (1DJL) (*12*, *37*), taking equivalent precautions to those outlined above for the crystallization of *R. rubrum* dI_2dIII_1 complexes. A complete data set was collected to 2.3 Å and processed as outlined above. The human dIII structure with bound $NADP^+$ was refined against the structure factor amplitudes of dIII with bound NADPH using the program CNS (*38*).

The absorbance spectra of single crystals were recorded on the microspectrophotometer described (*39*). The crystals, supported on goniometer loops, were briefly washed by passing through a solution identical in composition to the mother liquor but containing no nucleotides and supplemented with 18% glycerol. Spectra were referenced against a similar solution.

Diagrams were constructed with the programs MOLSCRIPT (*40*), BOBSCRIPT (*41*), RASTER-3D (*42*), and GRASP (*43*).

RESULTS AND DISCUSSION

Crystal Structures of dI_2dIII_1 Complexes with Bound NAD^+ and $NADP^+$. We suggested that NAD^+ binding to the dI(B) polypeptide of the dI_2dIII_1 complex is not as strong as to the dI(A) polypeptide. This would explain why the electron density in the binding site of the former is much weaker than that in the latter in crystals grown in 5 mM NAD^+ and 5 mM $NADP^+$ [PDB 1HZZ (*15*)]. However, the point is difficult to prove directly because the dissociation constants for NAD^+ are very high and measurements are therefore inaccurate [e.g., the K_d of the isolated dI dimer for NAD^+ is ∼300 μM (*44*)]. An important objective is to study the hydride-transfer site at the dI(B)−III interface of transhydrogenase, and therefore in the present work, we sought to increase occupation of dI(B) in the complex by growing crystals at elevated concentrations of NAD^+ (50 mM) while keeping the $NADP^+$ at 5 mM. Good crystals, diffracting to 2.3 Å, were obtained with otherwise only minor changes in growth conditions, and the structure was solved by molecular replacement (Table 1).

The fold of the new structure (PDB designation 1U28) is very similar to that of 1HZZ (a set of PDB file listings of transhydrogenase components is presented in Table 2). The dIII polypeptide and its bound $NADP^+$ are in almost identical conformations (0.74 Å RMS deviation for 174 equivalent pairs of C_α atoms). However, there are differences between 1HZZ and 1U28 in the nucleotide-binding sites of both of the dI polypeptides. There is the hoped for improvement in nucleotide electron density in dI(B) reflecting the predicted increase in site occupancy, although not all of the NAD^+ molecule is ordered. The adenosine and pyrophosphate groups are in satisfactory density, but the nicotinamide and nicotinamide−ribose cannot be discerned. Thus, again we are unable directly to visualize the nucleotides in their hydride-transfer positions. Note that it is necessary to have both nucleotides in the same oxidation state during crystallization to prevent hydride transfer, and the juxtaposition of the positively charged nicotinamide rings of both NAD^+ and $NADP^+$ may be a factor that contributes to perturbation of the site. Apparent movements of the nicotinamide mononucleotide moiety of the NAD(H) are a feature revealed also

Table 2: Crystal Structures of Isolated dI and dIII Components and dI_2dIII_1 Complexes of Transhydrogenases

species	protein	ligand (mM)[a]	polypeptides in the asu[b]	spacegroup (resolution, Å)	conformation of nic ring of NAD(H)[c]	PDB code	ref
R. rubrum	isolated dI	NAD^+ (10)	A	$P12_11$ (2.00)	distal/*syn*	1F8G	*13*
			B		disordered		
			C		disordered		
			D		proximal/*anti*		
R. rubrum	isolated dI	NADH (5)	A	$P12_11$ (1.90)	distal/*anti*	1L7E	*16*
			B		disordered		
			C		disordered		
			D		distal/*anti*		
R. rubrum	isolated dI	none	A, B, C, D	$P12_11$ (1.81)		1L7D	*16*
human	isolated dIII	$NADP^+$ (0)[e]	two	$P4_122$ (2.00)		1DJL	*12*
bovine	isolated dIII	$NADP^+$ (unavailable)[f]	one	$P1$ (1.21)		1D4O	*11*
human	isolated dIII	NADPH (5)	two	$P4_122$ (2.30)		1U31	*d*
human	isolated dIII	s-$NADP^+$ (5)	two	$P4_122$ (2.42)		1PT9	*18*
R. rubrum	isolated dIII	$NADP^+$ (unavailable)	two	$P6_122$ (2.10)		1PNO	*19*
R. rubrum	isolated dIII	NADPH (unavailable)	two	$P6_122$ (2.40)		1PNQ	*19*
R. rubrum	dI_2dIII_1	NAD^+ (5)	dI(A)	$P2_12_12_1$ (2.50)	distal/*anti*	1HZZ	*15*
	complex	$NADP^+$ (5)	dI(B)		disordered		
			dIII				
R. rubrum	dI_2dIII_1	NAD^+ (50)	dI(A)	$P2_12_12_1$ (2.30)	distal/*anti* + *syn*	1U28	*d*
	complex	$NADP^+$ (5)	dI(B)		disordered		
			dIII				
R. rubrum	dI_2dIII_1	NADH (50)	dI(A)	$P2_12_12_1$ (3.00)	distal/*anti*	1U2D	*d*
	complex	NADPH (5)	dI(B)		proximal/*anti*		
			dIII				
R. rubrum	dI_2dIII_1	ADPR (50)	dI(A), dI(B), dIII	$P2_12_12_1$ (2.20)		1U2G	*d*
	complex	NADPH (5)					
R. rubrum	dI_2dIII_1	s-NAD^+ (5)	dI(A)	$P2_12_12_1$ (2.61)	distal/*anti*	1PTJ	*18*
	complex	$NADP^+$ (5)	dI(B)		disordered		
			dIII				
R. rubrum	dI_2dIII_1	NAD^+ (5)	dI(A)	$P2_12_12_1$ (2.40)	distal/*anti*	1NM5	*17*
	complex	$NADP^+$ (5)	dI(B)		disordered		
	(dI·Q132N)		dIII				

[a] The ligand concentration in the crystallization drop is shown in parentheses. [b] The A polypeptides of all dI_2dIII_1 complexes are structurally equivalent with reference to the position of the dIII polypeptide (e.g., see Figure 1) and, similarly, the B polypeptides of all dI_2dIII_1 complexes. However, there is no implied equivalence between the A (or B) polypeptides of the dI_2dIII_1 complexes and the A (or B) polypeptides of isolated dI proteins; the designations were employed only for descriptive convenience. [c] The conformation of the (dihydro)nicotinamide ring of NAD(H) is described as distal or proximal to the NADP(H)-binding site, as described in the text. The terms *syn* and *anti* refer to the relative orientations of the nicotinamide and ribose rings around the glycosidic bond; see ref *45*. [d] This work. [e] Ligand tightly bound to protein from purification procedure. [f] Unavailable = not given in the cited reference.

in other structures described below, and their significance will be discussed later.

The electron density of the bound NAD^+ in the dI(A) polypeptide of 1HZZ indicates that the 3-carboxamide group of the nicotinamide ring is *anti* relative to the ribose (the glycosidic bond dihedral, X_n, = −145°). However, in 1U28 two protuberances of density probably associated with the carboxamide group of the nicotinamide ring of the NAD^+ in dI(A) suggest that both *anti* (X_n = −123°) and *syn* (X_n = 42°) conformations are possible (Figure 2). Simulated annealing omit maps (not shown) confirmed the positions of these protuberances. The difference in the electron density profiles of 1U28 and 1HZZ may be due to either the higher resolution or the switch from CNS to REFMAC for the refinement of the latter. The two values of X_n are both in the ranges commonly found for *anti* and *syn* conformations of NAD(P)(H) in other proteins (*45*). Analogous *anti* and *syn* conformations of the NAD^+ nicotinamide were observed in the crystal structure of isolated dI, 1F8G, though in different polypeptide chains (*13*). There are four polypeptides in the asymmetric unit of 1F8G (see Table 2): in polypeptide A, the nicotinamide is *syn*, in D the arrangement is *anti*, and in B and C the nicotinamide part is disordered (in all four the adenosine moieties are in good density). It is unusual

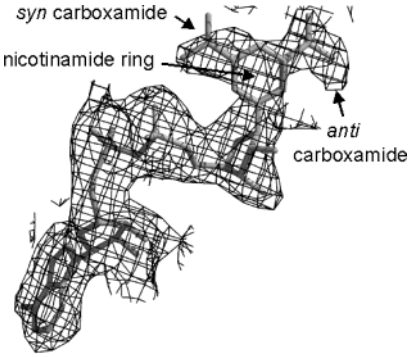

FIGURE 2: Electron density and atom coordinates of NAD^+ in the A polypeptide of the dI_2dIII_1 complex (PDB 1U28). The map (resolution 2.3 Å) is $2F_o - F_c$, SigmaA-weighted, and contoured at 1σ.

to find a protein that can bind nucleotides with both nicotinamide orientations. When poised for catalysis, the orientation determines whether the *pro-R* or *pro-S* hydrogen atom of $C4_N$ is transferred in the redox reaction, and by influencing the ring pucker, the site geometry of some soluble dehydrogenase enzymes is thought to activate the pseudoaxial hydride (*45*). Note, however, that the dI(A) polypeptide of the dI_2dIII_1 complex of transhydrogenase is thought to be

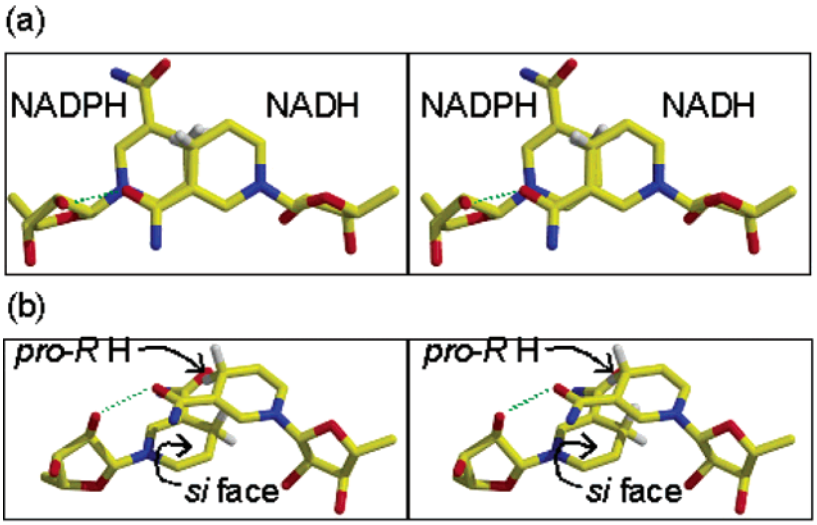

FIGURE 3: Stereoview of the apposed dihydronicotinamide rings of NADH and NADPH in the hydride-transfer site of the dI_2dIII_1 complex (PDB 1U2D). (a) The view is approximately normal to the plane of the nicotinamide rings. (b) The view is rotated to show how hydride transfer would lead to known stereochemistry. Color code: yellow, carbon; red, oxygen; blue, nitrogen; white, hydrogen. The green dotted lines show an H-bond between the carboxamide group of the NADH nicotinamide and the 2′-OH of the NADPH ribose.

locked in the open state (*4*, *5*, *15*) where, importantly, the hydride-transfer reaction must be switched off. A crucial feature of the open state is that the $C4_N$ of the NADH on dI and the $C4_N$ of the $NADP^+$ on dIII are held apart (to beyond hydride-transfer distance): whether the rings are bound in *anti* or *syn* conformations at this stage is therefore not critical to the proposed reaction mechanism (contrast this with the occluded state; see below). We suggest that the nicotinamide mononucleotide moiety of NAD^+ in the open state of transhydrogenase is weakly bound (the adenosine moiety provides most of the binding energy) and, when the protein is in aqueous solution, the nicotinamide ring can flip between the *anti* and *syn* forms. The conformation of the carboxamide group in dI(A) of 1HZZ is also unusual in that the $O7_N$ atom is *cis* to $C2_N$ (*18*), and the H-bonding pattern of the *anti* form of dI(A) of 1U28 indicates a similar organization. In the *syn* form, the conformation of the carboxamide group is not determined at this resolution.

Crystal Structures of dI_2dIII_1 Complexes with Bound NADH and NADPH: Nucleotide Conformations during Hydride Transfer. Measurements by microcalorimetry suggest that the dI(A) polypeptide of the dI_2dIII_1 complex binds NADH quite tightly ($K_d \approx 20$ μM) and the dI(B) binds the nucleotide rather more weakly ($K_d \approx 300$ μM) (*24*). The dIII component binds $NADP^+$ and NADPH extremely tightly ($K_d < 1$ nM), the reduced nucleotide somewhat more tightly than the oxidized (*31*). Crystals of the complex grown in the presence of 50 mM NADH and 5 mM NADPH had good electron density for nucleotide in all three polypeptides (Table 1, PDB code 1U2D). NADH and NADPH are not completely stable at neutral pH, but we conclude that those in the structure do represent the undegraded nucleotides. (1) Optical spectra of single crystals (obtained with the help of Dr. I. Clifton, University of Oxford) revealed a broad absorbance peak at approximately 330 nm, indicating reduced nicotinamide nucleotide (data not shown). The peak position was significantly greater than the wavelength (~310 nm) at which high levels of scattering by the crystals led to stray light distortion of the spectra (*39*). (2) NAD(P)H decomposition in aqueous solution leads to irreversible opening of the nicotinamide ring (*46*). Simulated annealing omit maps, however, establish that the nucleotides in the dI and dIII binding sites have intact ring structures in the nicotinamide region (not shown). The nucleotide is probably more resistant to degradation when bound within the protein environment.

This is the first instance of a crystal structure of a dI_2dIII_1 complex of transhydrogenase with all three nucleotide-binding sites occupied. The clearly defined densities of the NADH and NADPH at the dI(B)−dIII interface of the dI_2-$dIII_1$ complex reveal the structural basis for the known "A−B" stereochemistry of the redox reaction in transhydrogenase (*47*, *48*) and show how hydride transfer between the nucleotides can proceed directly without the participation of redox intermediates (*49*). Figure 3a illustrates the organization of the two dihydronicotinamide rings in the site. The NADH dihydronicotinamide is in an *anti* conformation, whereas that of the NADPH is *syn*. The carboxamide group of the NADH is within H-bonding distance of the 2′-OH of the N-ribose ring of the NADPH. The planes of the two dihydronicotinamide rings are approximately parallel. The rings do not stack face to face but are offset from one another such that the $C4_N-C5_N$ bond of the NADPH stacks against the $C3_N-C4_N$ bond of the NADH, and the $N1_N-C6_N$ and $C5_N-C6_N$ bonds of the NADPH stack against the 3-carboxamide group of the NADH. This arrangement brings the two $C4_N$ atoms into apposition, close enough (3.6 Å) for direct hydride transfer between them. Because both nucleotides in the structure are reduced, there must be some distortion in the site geometry (from the extra H atom and loss of positive charge) when compared, for example, to that with bound NADH and $NADP^+$, the physiological substrates during forward transhydrogenation. Nevertheless, it is clear how the *pro-R* hydrogen of $C4_N$ of NADH can be transferred to the *si* face of $C4_N$ of $NADP^+$ (Figure 3b), thus yielding the experimentally observed A−B transfer between NAD(H) and NADP(H).

NAD(H) Conformational Changes Preceding and Following the Hydride-Transfer Reaction. The conformation of the NADH in dI(A) of 1U2D, the polypeptide that is not associated with a dIII, is distinctively different from that in

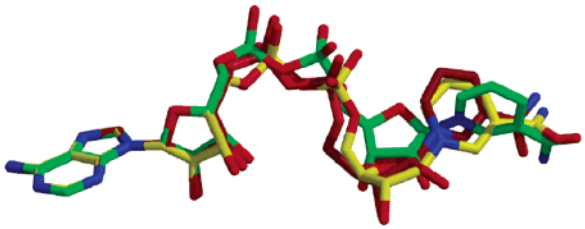

FIGURE 4: Conformations of the nicotinamide nucleotides bound to the dI_2dIII_1 complex. Nitrogen atoms are shown in blue and oxygen in red. The carbon and phosphorus atoms of NADH in polypeptide dI(B) of 1U2D are shown in green (a proximal structure; see text), those of NADH in dI(A) of 1U2D are in brown (a distal structure), and those of NAD^+ in polypeptide dI(A) of 1HZZ are in yellow (distal). The nucleotides were superimposed at the adenine group.

Table 3: Bond Rotations Involved in the Change in Conformation of NADH between the dI(A) and dI(B) Polypeptides of the dI_2dIII_1 Complex[a]

bond	rotation (deg)	bond	rotation (deg)
$N9_A-C1'_A$	2	$OP3-P_N$	25
$C1'_A-O4'_A$	2*	$P_N-O5'_N$	16
$O4'_A-C4'_A$	7*	$O5'_N-C5'_N$	27
$C4'_A-C5'_A$	13	$C5'_N-C4'_N$	4
$C5'_A-O5'_A$	4	$C4'_N-O4'_N$	27*
$O5'_A-P_A$	−17	$O4'_N-C1'_N$	16*
P_A-OP3	10	$C1'_N-N1'_N$	4

[a] The rotations are of the NADH bonds in dI(B) relative to those in dI(A). They are measured along the bond as viewed from the adenine end of the molecule in the 1U2D structure. A positive value is a clockwise rotation of the atom closest to the nicotinamide ring with the atom closest to the adenine ring held fixed. The angles marked with the asterisk correspond to slight alterations in the ribose ring pucker and do not greatly affect the overall conformation of the nucleotide.

dI(B); see Figure 4. The adenine rings of the nucleotides are bound in a very similar manner in the two polypeptides, but the effect of cumulative small bond rotations, particularly in the pyrophosphate and ribose−phosphate regions (Table 3), leads to a large relative displacement of the dihydronicotinamide rings ($C4_N$ moves by about 2.9 Å). Remarkably, the conformation of the NADH in dI(A) of 1U2D is very similar to that of the NAD^+ seen in dI(A) of the 1HZZ structure of the dI_2dIII_1 complex (also shown in Figure 4). Modeling studies showed that $C4_N$ of nucleotide in this conformation at the hydride-transfer site would be too far from that of the NADP(H) on a partner dIII to permit a redox reaction; we designated this the "distal" organization (*17*, *18*). We proposed that, in its initial binding to the open state of dI in intact transhydrogenase, NADH adopts this conformation to prevent the redox reaction with $NADP^+$ from occurring in the absence of proton translocation. When the enzyme is driven into its occluded state by protonation/deprotonation reactions associated with translocation, the dihydronicotinamide and nicotinamide rings are moved toward each other to switch on hydride transfer. In 1HZZ the dI(B) site was empty, and we could only guess at the nature of the movement. A modeling exercise showed that apposition could be achieved by rotating the dihydronicotinamide ring of NADH into a proximal position for hydride transfer (*15*). The 1U2D structure now provides strong supporting evidence for this suggestion: the electron density for the NADH in dI(B) shows that the dihydronicotinamide ring is close to the "proximal position" postulated in ref *17*, and it shows that interconversion with the distal dihydronicotinamide ring position in dI(A) can be achieved by the bond rotations described in Table 3.

There are now three crystal structures of the wild-type dI_2dIII_1 complex of *R. rubrum* transhydrogenase which are either completely or partially loaded with physiological nucleotides (1U28, 1U2D, and 1HZZ) and two of the isolated dI protein (the NAD^+-bound form, 1F8G, and the NADH-bound form, 1L7E); each of the isolated dI structures has four polypeptides in the asymmetric unit (asu); see Table 2. It is instructive to compare the dI structures on the basis of the conformation of the bound nucleotides (i.e., whether proximal or distal as defined above and illustrated in Figure 4). Three categories can be recognized: (1) those where the electron density for the adenosine moiety is quite clear but that for the nicotinamide moiety is weak, a feature that presumably reflects structural disorder at this end of the bound ligand (this category includes the B polypeptide of 1U28 and the B and C polypeptides of 1F8G); (2) those with all of the bound ligand in good density and where the (dihydro)nicotinamide is in the proximal position (the B polypeptide of 1U2D and the D polypeptide of 1F8G); and (3) those with all of the bound ligand in good density and where the (dihydro)nicotinamide is in the distal position (the A polypeptides of 1HZZ, 1U28, and 1U2D, the A polypeptide of 1F8G, and the A and D polypeptides of 1L7E). Now when the structures of the dI polypeptides are superimposed, it is found that there is a difference in the domain organization between those having nucleotide in the proximal conformation and those having nucleotide in the distal conformation. In the former, the cleft (Figure 1) between the two domains of dI (denoted dI.1 and dI.2) is distorted as the result of a rotation of dI.1 relative to dI.2. Analysis by the program DYNDOM (*50*) shows that the rotation comprises both closure and twist components and that the bending amino acid residues and hinges are located in the two long α helices which link dI.1 and dI.2 (S141−Y146 in α6 and G319−A328 in α11; see Figure 3 in ref *5*). From this correlation, we suggest that the interdomain rotation is the cause of the distal−proximal movement of the NAD(H) nicotinamide which we believe is crucial for the hydride-transfer switch. The core of dI.1 is exceptionally rigid and conformationally homogeneous (*51*). Its movement relative to dI.2 will lead to compression of the "RQD loop" (residues 126−136), which lines the cleft and provides numerous contacts with the (dihydro)nicotinamide ring of NAD(H), shifting the ring between its distal and proximal positions. In solution, NADH binds to isolated *R. rubrum* dI with a single K_d of about 20 μM (two nucleotides per dimer) (*24*). If there is any cooperativity between the two sites, it falls within the experimental and systematic error of the measurement (perhaps ±5 μM). However, during crystallization of isolated dI, packing forces cause different relative rotations of dI.1 and dI.2 in the four subunits of the asu, and we suggest that this differentially affects the conformation of the bound nucleotide. Superimposition of the four polypeptides of the asu of apo-dI (1L7D) shows equivalent arrangements of dI.1 and dI.2 to those in the NAD^+− and NADH−dI structures (1F8G and 1L7E, respectively), indicating the primacy of the domain organization in determining the nucleotide conformation and the propensity toward asym-

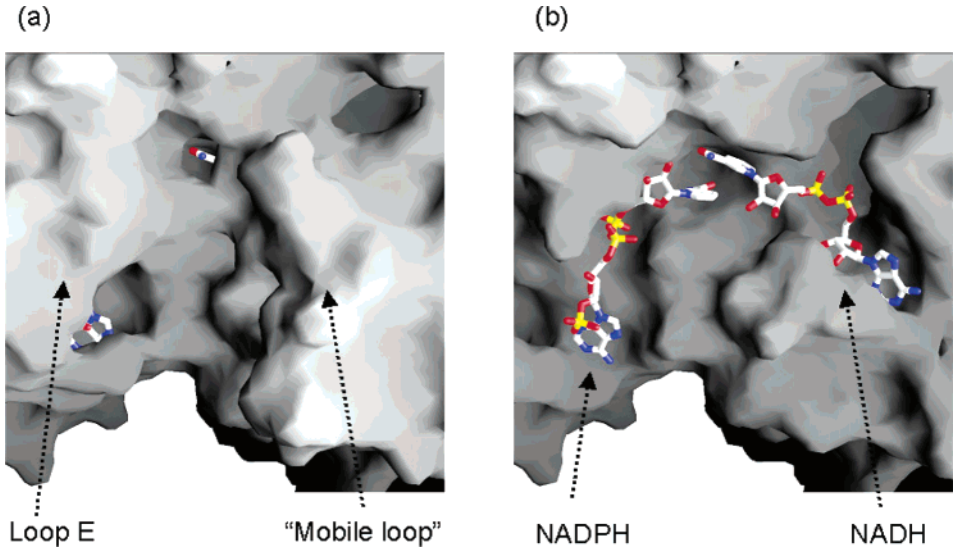

FIGURE 5: Bound nucleotides are occluded by the mobile loop of dI and loop E of dIII in the dI_2dIII_1 complex. (a) A surface representation of the interface of the dI(B) and dIII polypeptides. (b) The same view but with amino acid residues 221−247 (the mobile loop) of dI(B) and residues 161−178 (loop E) of dIII removed. NADH and NADPH are shown in stick format.

metry in the physiological dI dimer. In dI_2dIII_1 complexes, asymmetry is imposed on the dI protein by the interaction with the single, occluded-state dIII polypeptide even in aqueous solution: this, we suggest, can account for the different measured affinities of dI(A) and dI(B) for NADH that were referred to above. All crystal structures of dI_2dIII_1 complexes [including that of $(dI{\cdot}Q132N)_2dIII_1$, 1NM5, and that of wild-type proteins loaded with thio-NAD^+ and $NADP^+$, 1PTJ] reveal equivalent differences in the relative organization of dI.1 versus dI.2 in the two dI polypeptides. The implications of these structural features of the dI_2dIII_1 complex to the mechanism of proton translocation by intact transhydrogenase will be discussed in a later section.

Protein Rearrangements at the Hydride-Transfer Site. In the NMR spectrum of dI, resonances from the long loop comprising amino acid residues 223−239 are narrower than those from other parts of the molecule, showing that this segment of the polypeptide chain is relatively mobile in the solution state (*52*). Upon nucleotide binding to dI, these resonances shift and broaden, indicating that the "mobile loop" closes down on the protein surface. Consistent with this, the electron density of the feature in X-ray structures is generally much better when the binding site is occupied with NAD^+ or NADH. Where the density is good, the loop can be seen to extend from dI.2 across the cleft and contact R127 in the RQD loop of dI.1, thus shielding the bound nucleotide from the solvent. The mobile loop could be traced only partially and only in the A polypeptide of the earlier structure of the dI_2dIII_1 complex (1HZZ), but it is quite clear in both polypeptides of the new structure, 1U2D: the backbone of the loop is very similar to that observed in isolated dI (that is, in all four polypeptides of 1F8G and in the A and D polypeptides of 1L7E). At the dI(B)−dIII interface of 1U2D(B), the loop lies close to, but does not contact, amino acid residues and NADPH in dIII. A surface representation to show how the loop covers the bound NADH is shown in Figure 5.

A comparison of the available structures of dI indicates that nucleotide binding, movement of the R127 side chain, and closure of the mobile loop are coupled events. In isolated apo-dI (1L7D), R127 can adopt several different conformations, but in all cases the side chain either protrudes into the solvent or lies along the cleft opening between dI.1 and dI.2. Both the narrow line width in the NMR experiments and the lack of density in the crystal structure reveal the segmental flexibility of the mobile loop in this form of the protein (see above). Upon NAD^+ or NADH binding, the R127 side chain is drawn more deeply into the cleft. In the nine dI polypeptides having bound NAD(H) and where the electron density for these features is good enough for model building (polypeptides A−D of 1F8G, polypeptides A and D of 1L7E, the A polypeptide of 1HZZ, and the A and B polypeptides of 1U2D), the side chain of R127 contacts both Y235 (located near the apex of the mobile loop) and the nucleotide (via its guanidinium group and the nucleotide diphosphate, or the nicotinamide ribose, or both), e.g., Figure 6. Evidently, the bound nucleotide, the inwardly directed side chain of R127, and the mobile loop form a tightly interacting unit.

In the two structures that we identified above as having a proximally positioned (dihydro)nicotinamide ring (polypeptide D in 1F8G and polypeptide B in 1U2D), the R127 side chain lies much deeper in the cleft than in the structures characterized by distal NAD(H). Thus in 1F8G(D), the guanidinium group of the side chain makes H-bonds with the carboxylate of D135 and with hydroxyl group of S138, and in 1U2D(B), where the proximal nucleotide is oriented for the redox reaction with nucleotide bound to dIII, it makes two H-bonds to the carboxylate of D135. The side chains are in similar positions in these two structures, but small changes in their rotation have led to a different H-bonding organization. We suggest that the movement of the (dihydro)-nicotinamide of the NAD(H) from the distal to the proximal position is coupled to a deeper inward movement of the R127 side chain. It is envisaged that, as dI.1 moves against dI.2 (see above), the (dihydro)nicotinamide ring is pushed toward the rim of the cleft into the proximal position ready for hydride transfer and that this permits the R127 side chain to be drawn deeper into the cleft where it is stabilized by the formation of the charged H-bonds with D135 (compare

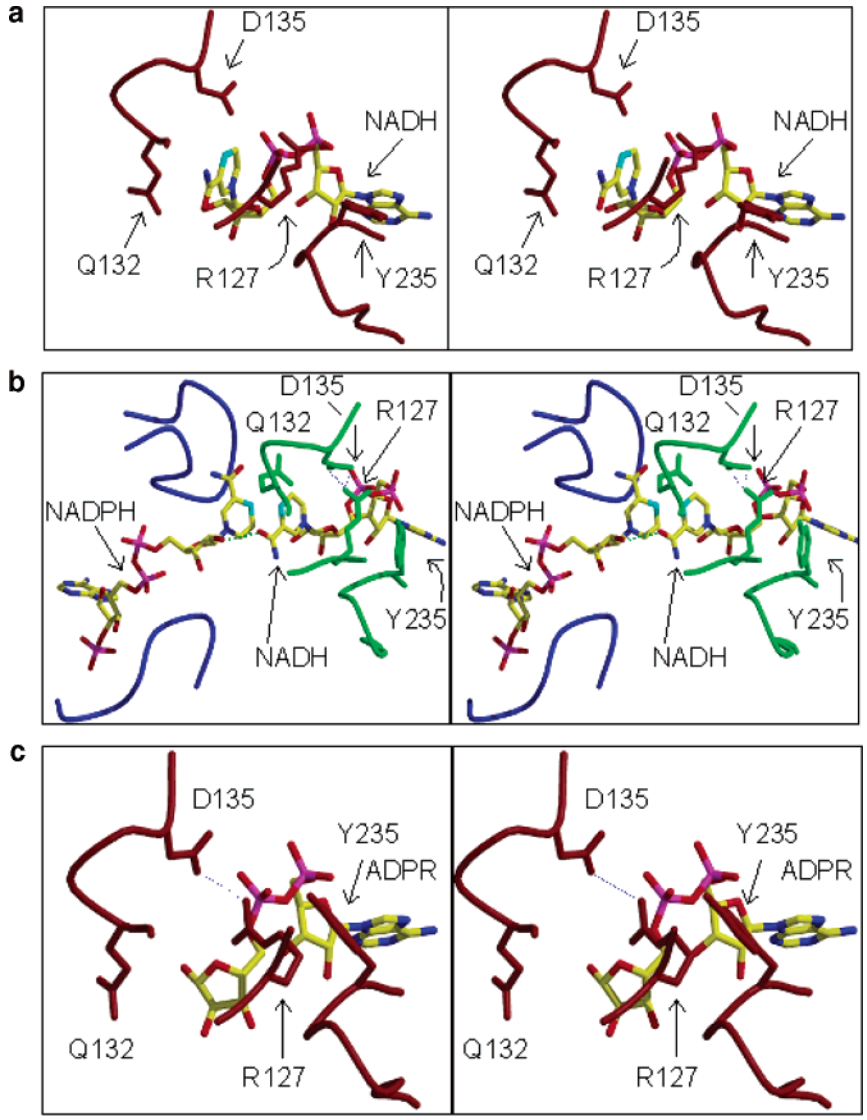

FIGURE 6: Stereoviews of the nucleotide-binding sites of dI_2dIII_1 complexes. (a) The NADH-binding site in the dI(A) polypeptide of 1U2D. The nucleotide is shown in the atom colors described in Figure 3 (in addition, $C4_N$ is in cyan and phosphorus is in purple) and the protein (main chain and side chains) is in brown. (b) The NADH- and NADPH-binding sites at the dI(B) and dIII polypeptides of 1U2D. The main chain of the dIII polypeptide is in blue, and the main chain and side chains of dI(B) are in green. (c) The ADPR-binding site of dI(A) of 1U2G. The main chain and side chains are in brown. Hydrogen bonds mentioned in the text are shown as either blue dotted lines (between amino acid side chains) or green dotted lines (between nucleotides).

panels a and b of Figure 6). Also consistent with this view, R127 adopts its deep-lying position and forms an H-bond with D135 in the B polypeptide of 1HZZ; although the electron densities for the nicotinamide of the bound NAD^+ and the mobile loop are weak, this is the dI polypeptide in the complex which, through its interaction with dIII, would be expected to drive the nicotinamide into the proximal position ready for hydride transfer.

The deeper movement of the R127 side chain that we suggest is associated with the distal → proximal conversion also appears to be correlated with a change in the Y235 conformation, and this too may have mechanistic significance. In dI(A) of 1U2D (distal NADH nicotinamide) the position of R127 and that of P268 (in the so-called TAGP loop; see ref 5) maintain Y235 in a rotamer which turns the aromatic side chain back toward the stem of the mobile loop (Figure 6a). In dI(B) the organization is more compact (proximal NADH nicotinamide). As the R127 side chain migrates deeper into the cleft and forms its new H-bonds with D135, the residue retains van der Waals contact with the tyrosine ring of Y235. The latter is then stabilized in a different rotamer in which the tyrosine ring arches over the NAD(H)-binding site (Figure 6b). We propose that this seals the site and helps to exclude water in preparation for hydride transfer. Again, a comparison with other dI structures supports the idea that this is a coupled motion. Thus, in the A polypeptide of isolated 1L7E and in the A polypeptide of the complex 1HZZ, where in both cases the (dihydro)-nicotinamide is distal and the R127 side chain is only slightly drawn into the cleft, the tyrosine ring of Y235 is turned back toward the stem of the mobile loop. However, in polypeptides B, C (no density for the nicotinamide), and D (proximal nicotinamide) of 1F8G and in polypeptide B of 1HZZ ("expected" to be proximal; see above), where the R127 side chain is deep in the cleft, the Y235 tyrosine ring is arched over the hydride-transfer site. The correlation cannot be extended to polypeptide D of 1L7E and polypeptide A of 1F8G because the improbably short distances between Y235

and adjacent atoms indicate that the chain was not properly traced through the rather weak density in this part of the mobile loop. The importance of Y235 is suggested by the fact that substitution with either phenylalanine or asparagine residues led to a 2−4-fold increase in the K_d for NADH binding by isolated dI and to pronounced inhibition of hydride transfer in intact transhydrogenase (*53*, *54*).

There appear to be somewhat equivalent interactions to those described for dI between arginine and tyrosine residues and the (dihydro)nicotinamide ring at the NADP(H)-binding site in dIII. Here, R90 from the nicotinamide-binding loop forms H-bonds with the nucleotide pyrophosphate and intercalates between Y55 and the nicotinamide ring. The tyrosine ring of Y171 in the loop E "lid" (which appears to share similar features to the mobile loop of dI) also interacts with the nicotinamide ring and with R90. Loop E of dIII covers bound NADP(H) in the same way that the mobile loop of dI covers bound NAD(H); see Figure 5. Polarization of the nucleotides by the arginine residues at both sites, enhanced by the local low dielectric constant imposed by the adjacent tyrosine residues, may contribute to the distorted equilibrium constant ($K > 36$) for the redox reaction in the occluded state by destabilizing the substrate nucleotides and stabilizing the products (*26*).

In 1HZZ the side chain of Q132 in the RQD loop of dI-(B) can be seen to stretch across the interface with dIII and make an H-bond with the 2′-OH group of the $NADP^+$ ribose. We suggested that this might provide a means to "tether" the nucleotides prior to the hydride-transfer step (*17*). In support of this proposal, substitution of Q132 with an asparagine residue resulted in loss of the apparent H-bond with the $NADP^+$ ribose at the dI(B)−dIII interface of an X-ray structure and an ∼1000-fold decrease in the rate constant for hydride transfer measured in stopped-flow experiments. In dI(B) of 1U2D, where the nucleotide-binding site is occupied by NADH with its dihydronicotinamide in a proximal position, the side chain of Q132 is rotated about its $C_\alpha-C_\beta$ bond, and this results in its amide group folding back into H-bond contact with invariant S138 and into van der Waals contact with the *si* face of the dihydronicotinamide ring (Figure 6b). A very similar organization is observed in the other structure with nucleotide in the proximal position (i.e., polypeptide D in 1F8G where, of course, the nucleotide is in the oxidized form and there is no associated dIII). In almost all other dI polypeptides [including dI(A) of 1U2D; see Figure 6a] the Q132 side chain is in the extended conformation. The only exception is 1HZZ(A), where the residue adopts an intermediate form, but note that, in the somewhat equivalent 1U28(A), Q132 is extended. The indications are therefore that Q132 moves from its fully extended to its fully folded back conformation when the (dihydro)nicotinamide ring of the NAD(H) moves into the proximal position. The movement of the Q132 side chain appears to be necessary to allow displacement of the NAD(H) (dihydro)nicotinamide between the distal and proximal positions without clashing. We suggest, therefore, that Q132 tethers the RQD loop of dI to the NADP(H) ribose in preparation for the dI.1/dI.2 interdomain movement that drives the distal-to-proximal shift of the (dihydro)nicotinamide ring of the NAD(H) but that, as the shift occurs, the nicotinamide displaces the Q132 side chain into the folded back conformation. The close interaction between the amide group of Q132 in the folded back conformation and the NAD(H) (dihydro)nicotinamide ring may contribute to important polarization changes in the nucleotides during hydride transfer (see above). Thus, the amide group of Q132 is located only a short distance (∼3 Å) from the $C4_N$ of the NADH and is involved in a network of H-bonds with D135 and S138.

Crystal Structure of dI_2dIII_1 Complexes with Bound ADP-ribose (ADPR) and NADPH. To investigate further the suggestion that the distal-to-proximal movement of the (dihydro)nicotinamide ring in dI is coupled to side-chain movements of amino acid residues in the RQD loop, the dI_2-$dIII_1$ complex was crystallized in the presence of 50 mM ADPR and 5 mM NADPH. The X-ray structure was solved to 2.2 Å resolution (Table 1) and is designated 1U2G in the PDB. ADPR is NAD(H) with its (dihydro)nicotinamide group hydrolytically removed at the glycosidic bond. There is good electron density for NADPH in dIII and for ADPR in both dI(A) and dI(B). It is clear that the adenosine moiety binds to both polypeptides in the same way that the adenosine of NAD(H) is bound in the previously described structures. In both the dI(A) and dI(B) polypeptides the "nicotinamide" ribose group of the ADPR occupies slightly different positions from those in the NAD(H) structures presumably because constraints resulting from interactions between the nicotinamide and the protein are lost. As expected, there is no electron density in the nicotinamide-binding pocket that can be attributed to the presence of atoms from the ligand.

As in all other X-ray structures of dI_2dIII_1 complexes, the shape of the cleft of dI(B) in 1U2G is slightly different from that in dI(A). This supports the suggestion that the movement of dI.1 against dI.2 in the B polypeptide is determined by the bound dIII, and it is consistent with the idea that this is the motion that leads to the distal-to-proximal shift in the nicotinamide nucleotide conformation. The opposite view, that asymmetries in the dI dimer (e.g., resulting from the interaction with dIII) force the (dihydro)nicotinamide of bound NAD(H) into proximal and distal positions and that this causes the movement of dI.1 against dI.2, is untenable.

As in the structure of the complexes with bound NAD^+ and $NADP^+$ (1HZZ and 1U28), the electron density of the mobile loop is better in the A polypeptide of 1U2G (Figure 6c) than in the B polypeptide. The fact that there is good density for the loop in at least one of the subunits indicates that its closure does not require the presence of the nicotinamide ring. In 1U2G and in all other dI structures having good density for the mobile loop, there is contact between A236 and the adenine rings of the bound nucleotide: in 1U2G, this is the only contact between the loop and the nucleotide but in dI with either bound NAD^+ or bound NADH there are additional interactions between Y235 and the nicotinamide mononucleotide moiety (see above). In earlier work, it was shown that substituting A236 with glycine had only a partial inhibitory effect on the rate of hydride transfer in intact transhydrogenase at saturating nucleotide concentrations but that it substantially lowered the affinity of isolated dI for NADH (the K_d was increased >10-fold) and increased the concentration of nucleotide required to broaden the mobile loop resonances in NMR experiments (*55*). Mutations in other amino acid residues in the mobile loop (including Y235; see above) led to much smaller effects on the NADH-binding affinity. It is therefore

suggested that the A236 contact with the adenine group is important during loop closure over the dI cleft but that, once the loop has closed (through interactions between Y235 and the bound nucleotide), the redox reaction can proceed at a substantial rate.

An important finding is that in dI(A) of 1U2G the side chain of R127 is inserted deep into the cleft between dI.1 and dI.2 with its guanidinium group in H-bond contact with D135 (Figure 6c). As described above, this organization is observed only in the two nicotinamide-proximal structures (the B polypeptide of 1HZZ and the D polypeptide of 1F8G). We therefore conclude that it is the absence of the (dihydro)-nicotinamide ring from the distal position, and not the presence of a (dihydro)nicotinamide ring in the proximal position, that favors this organization. The fact that the R127 side chain is not located in its deep-lying position in isolated apo-dI (1L7D) shows that closure of the mobile loop (probably resulting from interactions between A236 and the adenine ring system; see above) and the consequent interactions between Y235, R127, and the nucleotide are necessary for the stabilization of this configuration. Consistent with the corollary developed in the previous section, the tyrosine ring of Y235 is pulled down by its interaction with the deep-lying R127 and thus arches over and more completely seals the site (Figure 6c).

The side chain of Q132 is in its extended conformation in both the A and the B polypeptides of 1U2G. Thus, in the latter it reaches across the dI(B)−dIII interface and makes H-bond contact with the nicotinamide−ribose of the bound NADPH, and in the former (Figure 6c) it protrudes into the solvent. This supports the above suggestion that Q132 adopts its folded back conformation only when the NAD(H) binding site is occupied by a (dihydro)nicotinamide group in the proximal position.

Crystal Structure of Human dIII with Bound NADPH. The solution structure of isolated *R. rubrum* dIII in its $NADP^+$ form was solved by NMR spectroscopy (*14*). When bound $NADP^+$ was replaced with NADPH in this protein, pronounced chemical shift changes of backbone amide groups were revealed in an HSQC experiment, not just in the (dihydro)nicotinamide binding pocket, but also in a spur of amino acids that extends unidirectionally into helix D/loop D and loop E (*27*). Similar changes were later observed in isolated *E. coli* dIII (*56*, *57*). In both cases the chemical shift perturbations were taken as evidence either for changes in conformation or for polarization of amino acid residues resulting from the altered redox state of the nucleotide. However, in the work described above, it emerged that the crystal structure of the dIII component in dI_2dIII_1 complexes of *R. rubrum* transhydrogenase is remarkably similar when either $NADP^+$ or NADPH is bound. Furthermore, a new crystal structure of isolated dIII from *R. rubrum* transhydrogenase with bound $NADP^+$ (1PNO) is similar to that with bound NADPH (1PNQ) (*19*). We report here that the crystal structure of isolated human dIII with bound NADPH solved to a resolution of 2.3 Å (Table 1, 1U31) is similar to that with bound $NADP^+$ (1DJL**)** (*12*); the RMS deviation is 0.16 Å for 176 equivalent pairs of C_α atoms.

The prediction of structure changes from the chemical shift changes of substituent atoms in macromolecules is not yet a feasible exercise. However, it is clear from these recent crystal structures that the large chemical shift changes (in helix D/loop D and loop E) caused by exchanging $NADP^+$ with NADPH on dIII are unlikely to be the result of large atomic displacements. They might result from changes in the electrical polarization of amino acid residues in these secondary-structure features or from atomic displacements that are too small to be detected by X-ray crystallography at the presently available resolutions. However, the directionality and extent of the chemical shift changes across the dIII polypeptide may point to a mechanistic significance (see below).

Coupling between the Redox Reaction and Proton Translocation in Intact Transhydrogenase. We have shown (*15*, *21*, *22*, *31*, *58*, *59*) that the properties of the dI_2dIII_1 complex formed upon mixing recombinant dI and dIII [notably, the capacity for very high rates of hydride transfer at the dI(B)−dIII interface and the very low rates of release of bound $NADP^+$/NADPH] are, within the context of our binding-change mechanism, precisely what would be expected of a catalytic intermediate (the "occluded state") in the reaction. We had suggested that, in the absence of the membrane-spanning dII, the dI(B) and dIII polypeptides of the complex are *locked* in this occluded state, whereas in intact transhydrogenase proton translocation through dII would drive the enzyme *between* the occluded and open states. Recent mutagenesis experiments provide good evidence for an important feature of this mechanism (*60*). When βG252 in the dII component of the intact *E. coli* transhydrogenase is substituted with other amino acid residues, the mutant enzymes behave precisely like the isolated (wild-type) dI_2dIII_1 complex: they have the capacity for rapid hydride transfer, but rates of release of $NADP^+$ and NADPH from the enzyme are greatly retarded and the nucleotides remain tightly bound to the protein. These dII mutations appear to decouple hydride transfer from proton translocation and thus lock the peripheral components in the occluded state. The experiments therefore provide a valuable link between the work on the dI_2dIII_1 complex and that on the intact transhydrogenase; i.e., mutation of βG252 and "removal" of dII from the nucleotide-binding components have essentially the same effect. Substitution of βH91 and βN222, also in dII, with positively charged residues has a similar, though slightly more complex result (*61*). Somewhat surprisingly, substitution of βG252 in Cys-free, His-tagged *E. coli* transhydrogenase led to pronounced inhibition of hydride transfer (*62*). Hitherto it had been thought that the Cys-free, His-tagged enzyme had essentially wild-type properties. Why mutants of this protein variant should behave differently to those of the wild-type parent (*60*) is unclear, and it will be important to establish the reasons for the discrepancy.

The architecture of the intact transhydrogenase deduced from the crystal structure of the dI_2dIII_1 complex indicates that the hydride-transfer site is located some distance from the membrane (see Figure 1). The conformational changes that are generated by proton translocation through dII and that cause active-site opening/occlusion and gate the hydride-transfer step must therefore be transmitted across dIII (some 30 Å). We suggested that energy transmission probably involves loop E and helix D/loop D of dIII (*5*, *15*). Thus, movements of loop E were proposed to regulate the access of bound $NADP^+$ and NADPH to the solvent, and movements of the adjacent helix D/loop D were proposed to be important in driving the dI.1/dI.2 rotations that alter the

NAD(H) conformation (see above). Recently, two different conformations of loop D were observed in the X-ray structure of crystals of isolated dIII grown in 50% ^2H_2O (*19*). One conformation is very similar to that seen in all previous dIII structures, but in the other, the tip of loop D is moved by ~10 Å (toward the bound nucleotide), strongly supporting the view that this feature might indeed undergo a conformational change during turnover of the intact enzyme. Following the recognition that hydride transfer must be prevented in some reaction intermediates (*10*, *21*), the authors of this work suggested that, by covering the *si* face of the nicotinamide ring, the observed movement of loop D might be responsible for the necessary blockade of the redox reaction. However, we think that this is unlikely since their putative "blocked state" is a very closed structure (both helix D/loop D and loop E shroud the nucleotide) but it is in the *open* state of transhydrogenase (when product nucleotides are released and fresh nucleotides bind) that there is a requirement to prevent hydride transfer. Rather, the original suggestion, that movement of loop D causes the opening and closing of the dI cleft (*5*, *15*), is to be preferred. Thus, in all structures of dI_2dIII_1 complexes (Table 2) the tip of loop D contacts the highly conserved RQD loop of dI.1(B), and helices αA and αB on the other side of dIII, which are packed closely against the β sheet core, contact dI.2(B). Changes in the conformation of loop D of the type seen in ref *19* would therefore lead to the relative movements of dI.1(B) and dI.2(B) that influence the cleft region and the distal−proximal equilibrium.

The structures described in the present report provide further information on the probable events associated with hydride transfer in transhydrogenase. NADH binds with moderate affinity to isolated dI and to open-state dI(A) in the dI_2dIII_1 complex (*24*, *44*). Partial closure of the mobile loop accompanies the binding of this nucleotide independently of events in dII and dIII (*52*). Thus, the configuration of the bound NADH and protein observed in dI(A) of 1U2D (Figure 6a) is what we should expect in the intact enzyme immediately after nucleotide binding to that dI-dII-dIII monomer which is in the open state. NADH is in the distal position, and Y235 of the mobile loop only partly seals the site from the solvent. However, as dIII is shifted (by proton translocation through dII) into the occluded state, it begins to interact more strongly with dI. At an early stage in this process, Q132 of dI helps to tether the two sides of the active site. Conformational changes in helix D/loop D of dIII then drive the relative movements of dI.1 and d1.2, pushing the NADH dihydronicotinamide into the proximal position, allowing R127 to form the H-bond with D135 (Figure 6b) and thus pulling in the side chain of Y235 to completely seal the site (see above). The resulting reorganization of the site during this transition brings together the dihydronicotinamide and nicotinamide rings for hydride transfer. Simultaneously, through the redistribution of charged and polar amino acid side chains in the low local dielectric constant of the site, changes in the nucleotide-binding energies elevate K_{eq} and bias the reaction toward $NADP^+$ reduction. Redox equilibrium is reached very rapidly (*26*). Dissociation of product NAD^+ and NADPH will follow as the dI-dII-dIII monomer of the enzyme is driven back into the open state by further interaction with the proton translocating apparatus in dII.

We suggested that proton binding to the outside aqueous phase and proton release to the inside aqueous phase are the events in proton translocation that are coupled to the open → occluded and occluded → open transitions of intact transhydrogenase (*10*, *21*). It is therefore essential for the enzyme to switch access of the proton translocation device to either the inside or outside aqueous phases in concert with the redox reaction. Before the crystal structures were solved, we proposed that the redox state of the dIII-bound NADP(H) is probably the important determinant of proton access, and this still seems to us to be the most plausible mechanism. Clearly, the coordinating signal must be transmitted back across dIII to dII to have its effect. Information transmission need not involve large conformational changes, and it is possible that the magnetization changes that propagate through helix D/loop D and loop E, as observed in NMR experiments when $NADP^+$ is replaced by NADPH on the isolated dIII component (see above and refs *5* and *27*), are a manifestation of the signal.

In other membrane proteins, local changes in the orientation of amino acid side chains at the catalytic site are also expected to be associated with the larger scale conformational changes that are responsible for coupling the chemical transformation to solute/ion translocation (e.g., ref *63*). In some of these proteins, the character of the large-scale conformational change is established, but the relationship with events at the catalytic site is still far from clear. The fact that the dI_2dIII_1 complex of transhydrogenase can be loaded with redox-inactive combinations of nucleotides enables us to visualize microstates of the active site in some detail. There are likely to be similarities in the energy coupling mechanisms of different translocation proteins, and observations on structure changes of the dI_2dIII_1 complex may provide useful information on the fundamental principles of this process.

ACKNOWLEDGMENT

We are very grateful to Dr. Ian Clifton for help in recording the single-crystal spectra, to the staff at the European Synchrotron Radiation Facility at Grenoble for help in X-ray data collection, and to Nick Cotton for advice on protein expression and purification.

REFERENCES

1. Stock, D., Gibbons, C., Arechaga, I., Leslie, A. G., and Walker, J. E. (2000) The rotary mechanism of ATP synthase, *Curr. Opin. Struct. Biol. 10*, 672−679.
2. Locher, K. P., Lee, A. T., and Rees, D. C. (2003) The *E. coli* BtuCD structure: a framework for ABC transporter architecture and mechanism, *Science 296*, 1091−1098.
3. Toyoshima, C., Nomura, H., and Sugita, Y. (2003) Structural basis of ion pumping by Ca^{++}-ATPase by sarcoplasmic reticulum, *FEBS Lett. 555*, 106−110.
4. Jackson, J. B. (2003) Proton translocation by transhydrogenase, *FEBS Lett. 545*, 18−24.
5. Jackson, J. B., White, S. A., Quirk, P. G., and Venning, J. D. (2002) The alternating site, binding change mechanism for proton translocation by transhydrogenase, *Biochemistry 41*, 4173−4185.
6. Bizouarn, T., Fjellstrom, O., Meuller, J., Axelsson, M., Bergkvist, A., Johansson, C., Karlsson, G., and Rydstrom, J. (2000) Proton translocating nicotinamide nucleotide transhydrogenase from *E. coli*. Mechanism of action deduced from its structural and catalytic properties, *Biochim. Biophys. Acta 1457*, 211−218.
7. Rydstrom, J., and Hoek, J. B. (1988) Physiological roles of nicotinamide nucleotide transhydrogenase, *Biochem. J. 254*, 1−10.

8. Sazanov, L. A., and Jackson, J. B. (1994) Proton translocating transhydrogenase and NAD- and NADP-linked isocitrate dehydrogenases operate in a substrate cycle which contributes to the fine regulation of the tricarboxylic acid cycle activity in mitochondria, *FEBS Lett. 344*, 109−116.
9. Mercer, N. A., McKelvey, J. R., and Fioravanti, C. F. (1999) *Hymenolepis diminuta:* catalysis of transmembrane proton translocation by mitochondrial NADPH−NAD transhydrogenase, *Exp. Parasitol. 91*, 52−58.
10. Jackson, J. B., Peake, S. J., and White, S. A. (1999) Structure and Mechanism of proton-translocating transhydrogenase, *FEBS Lett. 464*, 1−8.
11. Prasad, G. S., Sridhar, V., Yamaguchi, M., Hatefi, Y., and Stout, C. D. (1999) Crystal structure of transhydrogenase domain III at 1.2 Å resolution, *Nat. Struct. Biol. 6*, 1126−1131.
12. White, S. A., Peake, S. J., McSweeney, S., Leonard, G., Cotton, N. N. J., and Jackson, J. B. (2000) The high-resolution structure of the NADP(H)-binding component of proton-translocating transhydrogenase from human-heart mitochondria, *Structure 8*, 1−12.
13. Buckley, P. A., Jackson, J. B., Schneider, T., White, S. A., Rice, D. W., and Baker, P. J. (2000) Protein−protein recognition, hydride transfer and proton pumping in the transhydrogenase complex, *Structure 8*, 809−815.
14. Jeeves, M., Smith, K. J., Quirk, P. G., Cotton, N. P. J., and Jackson, J. B. (2000) Solution structure of the NADP(H)-binding component (dIII) of proton-translocating transhydrogenase from *Rhodospirillum rubrum*, *Biochim. Biophys. Acta 1459*, 248−257.
15. Cotton, N. P. J., White, S. A., Peake, S. J., McSweeney, S., and Jackson, J. B. (2001) The crystal structure of an asymmetric complex of the two nucleotide-binding components of proton-translocating transhydrogenase, *Structure 9*, 165−176.
16. Prasad, G. S., Wahlberg, M., Sridhar, V., Sundaresan, V., Yamaguchi, M., Hatefi, Y., and Stout, C. D. (2002) Crystal structures of transhydrogenase domain I with and without bound NADH, *Biochemistry 41*, 12745−12754.
17. van Boxel, G. I., Quirk, P., Cotton, N. J. P., White, S. A., and Jackson, J. B. (2003) Glutamine-132 in the NAD(H)-binding component of proton-translocating transhydrogenase tethers the nucleotides before hydride transfer, *Biochemistry 42*, 1217−1226.
18. Singh, A., Venning, J. D., Quirk, P., van Boxel, G. I., Rodrigues, D. J., White, S. A., and Jackson, J. B. (2003) Interactions between transhydrogenase and thio-nicotinamide analogues of NAD(H) and NADP(H) underline the importance of nucleotide conformational changes in coupling to proton translocation, *J. Biol. Chem. 278*, 33208−33216.
19. Sundaresan, V., Yamaguchi, M., Chartron, J., and Stout, C. D. (2003) Conformational change in the NADP(H)-binding domain of transhydrogenase defines four states, *Biochemistry 42*, 12143−12153.
20. Hutton, M. N., Day, J. M., Bizouarn, T., and Jackson, J. B. (1994) Kinetic resolution of the reaction catalysed by proton-translocating transhydrogenase from *Escherichia coli* as revealed by experiments with nucleotide substrate analogues, *Eur. J. Biochem. 219*, 1041−1051.
21. Bizouarn, T., Stilwell, S. N., Venning, J. M., Cotton, N. P. J., and Jackson, J. B. (1997) The pH dependences of reactions catalysed by the complete proton-translocating transhydrogenase from *Rhodosprillum rubrum*, and by the complex formed from its recombinant peripheral, nucleotide-binding domains, *Biochim. Biophys. Acta 1322*, 19−32.
22. Venning, J. D., and Jackson, J. B. (1999) A shift in the equilibrium constant at the catalytic site of proton-translocating transhydrogenase: significance for a "binding-change" mechanism, *Biochem. J. 341*, 329−337.
23. Jenks, W. P. (1983) What is a coupled vectorial process?, *Curr. Top. Membr. Transp. 19*, 1−18.
24. Venning, J. D., Rodrigues, D. J., Weston, C. J., Cotton, N. P. J., Quirk, P. G., Errington, N., Finet, S., White, S. A., and Jackson, J. B. (2001) The heterotrimer of the membrane-peripheral components of transhydrogenase and the alternating-site mechanism of proton translocation, *J. Biol. Chem. 276*, 30678−30685.
25. Venning, J. D., Bizouarn, T., Cotton, N. P. J., Quirk, P. G., and Jackson, J. B. (1998) Stopped-flow kinetics of hydride transfer between nucleotides by recombinant domains of proton-translocating transhydrogenase, *Eur. J. Biochem. 257*, 202−209.
26. Pinheiro, T. J. T., Venning, J. D., and Jackson, J. B. (2001) Fast hydride transfer in proton-translocating transhydrogenase revealed in a rapid-mixing, continuous-flow device, *J. Biol. Chem. 276*, 44757−44761.
27. Quirk, P. G., Jeeves, M., Cotton, N. P. J., Smith, K. J., and Jackson, J. B. (1999) Structural changes in the recombinant, NADP(H)-binding component (dIII) of proton-translocating transhydrogenase revealed by NMR spectroscopy, *FEBS Lett. 446*, 127−132.
28. Phelps, D. C., and Hatefi, Y. (1984) Interaction of purified nicotinamidenucleotide transhydrogenase with dicyclohexylcarbodiimide, *Biochemistry 23*, 4475−4480.
29. Phelps, D. C., and Hatefi, Y. (1985) Mitochondrial nicotinamide nucleotide transhydrogenase: active site modification by 5′-(*p*-(fluorosulfonyl)benzoyl)adenosine, *Biochemistry 24*, 3503−3507.
30. Diggle, C., Hutton, M., Jones, G. R., Thomas, C. M., and Jackson, J. B. (1995) Properties of the soluble polypeptide of the proton-translocating transhydrogenase from *Rhodospirillum rubrum* obtained by expression in *Escherichia coli*, *Eur. J. Biochem. 228*, 719−726.
31. Diggle, C., Bizouarn, T., Cotton, N. P. J., and Jackson, J. B. (1996) Properties of the purified, recombinant, NADP(H)-binding domain III of the proton-translocating nicotinamide nucleotide transhydrogenase from *Rhodospirillum rubrum*, *Eur. J. Biochem. 241*, 162−170.
32. Peake, S. J., Venning, J. D., and Jackson, J. B. (1999) A catalytically active complex formed from the recombinant dI protein of *Rhodospirillum rubrum* transhydrogenase, and the recombinant dIII protein of the human enzyme, *Biochim. Biophys. Acta 1411*, 159−169.
33. Eklund, H., and Branden, C. I. (1987) Crystal structure, coenzyme conformations and protein interactions, in *Pyridine nucleotide coenzymes* (Dolphin, D., Poulson, R., and Avramovic, O., Eds.) pp 51−98, John Wiley and Sons, New York.
34. Leslie, A. G. W. (1992) Recent changes to the MOSFLM package for processing film and image data, *Jt. CCCP4 ESF-EADBM Newsl. Protein Crystallogr. 226*.
35. Evans, P. R. (1997) SCALA, *Jt. CCP4 ESF-EACMB Newsl. 33*, 22−24.
36. Murshudov, G. N., Vagin, A. A., and Dodson, E. J. (1997) REFMAC5, *Acta Crystallogr. D53*, 240−255.
37. Peake, S. J., Jackson, J. B., and White, S. A. (2000) The NADP-(H)-binding component of human-heart transhydrogenase: crystallization and preliminary crystallographic analysis, *Acta Crystallogr. D56*, 489−491.
38. Brunger, A. T., Adams, P. D., Core, G. M., DeLano, W. L., and Gross, P. (1999) Crystallography and NMR system: a new software suite for macromolecular structure determination, *Acta Crystallogr. D54*, 905−921.
39. Hadfield, A., and Hajdu, J. (1993) A fast and portable microspectrophotometer for protein crystallography, *J. Appl. Crystallogr. 26*, 839−842.
40. Kraulis, P. J. (1991) MOLSCRIPT: a program to produce both detailed and schematic plots of protein structure, *J. Appl. Crystallogr. 24*, 946−950.
41. Esnouf, R. M. (1997) An extensiviely modified version of MolScript that includes greatly enhanced coloring capabilities, *J. Mol. Graphics Modell. 15*, 132−134.
42. Merritt, E. A., and Bacon, D. J. (1997) Raster-3D photorealistic molecular graphics, *Methods Enzymol. 277*, 505−524.
43. Nicholls, A., Sharp, K. A., and Honig, B. (1991) Protein folding and association: insights from the interfacial and thermodynamic properties of hydrocarbons., *Proteins 11*, 281−296.
44. Bizouarn, T., Diggle, C., and Jackson, J. B. (1996) The binding of nucleotides to domain I proteins of the proton-translocating transhydrogenases of *Rhodospirillum rubrum* and *Escherichia coli* as measured by equilibrium dialysis, *Eur. J. Biochem. 239*, 737−741.
45. Almarrson, O., and Bruice, T. C. (1993) Evaluation of the factors influencing reactivity and stereospecificity in NAD(P)H dependent dehydrogenase enzymes, *J. Am. Chem. Soc. 115*, 2125−2138.
46. Oppenheimer, N. J. (1987) Chemical stability and reactivity of pyridine nucleotide coenzymes, in *Pyridine nucleotide coenzymes* (Dolphin, D., Poulson, R., and Avramovic, O., Eds.) pp 323−365, Wiley-Interscience, New York.
47. Lee, C. P., Simard-Duquesne, N., Ernster, L., and Hoberman, H. D. (1965) Stereochemistry of hydrogen transfer in the energy-linked pyridine nucleotide transhydrogenase and related reactions, *Biochim. Biophys. Acta 105*, 397−409.
48. Fisher, R. R., and Guillory, R. J. (1971) Resolution of enzymes catalyzing energy-linked transhydrogenation−Preparation and

properties of *Rhodospirillum rubrum* transhydrogenase factor, *J. Biol. Chem. 246*, 4687−4693.
49. Venning, J. D., Grimley, R. L., Bizouarn, T., Cotton, N. P. J., and Jackson, J. B. (1997) Evidence that the transfer of hydride equivalents between nucleotides by proton-translocating transhydrogenase is direct, *J. Biol. Chem. 272*, 27535−27538.
50. Hayward, S., and Berendsen, H. J. C. (1998) Systematic analysis of domain motions in proteins from conformational change; new results on citrate synthase and T4 lysozyme, *Proteins: Struct., Funct., Genet. 30*, 144−150.
51. Broos, J., Gabellieri, E., van Boxel, G. I., Jackson, J. B., and Strambini, G. (2003) Tryptophan phosphorescence spectroscopy reveals that a domain in the NAD(H)-binding component (dI) of transhydrogenase from *Rhodospirillum rubrum* has an extremely rigid and conformationally homogeneous protein core, *J. Biol. Chem. 278*, 47578−47584.
52. Quirk, P. G., Smith, K. J., Thomas, C. M., and Jackson, J. B. (1999) The mobile loop region of the NAD(H)-binding component (dI) of proton-translocating transhydrogenase from *Rhodospirillum rubrum*: complete NMR assignment and effects of bound nucleotides, *Biochim. Biophys. Acta 1412*, 139−148.
53. Diggle, C., Quirk, P. G., Bizouarn, T., Grimley, R. L., Cotton, N. P. J., Thomas, C. M., and Jackson, J. B. (1996) Mutation of Tyr235 in the NAD(H)-binding subunit of the proton-translocating nicotinamide nucleotide transhydrogenase of *Rhodospirillum rubrum* affects the conformational dynamics of amobile loop and lowers the catalytic activity of the enzyme, *J. Biol. Chem. 271*, 10109−10115.
54. Bizouarn, T., Grimley, R. L., Diggle, C., Thomas, C. M., and Jackson, J. B. (1997) Mutations at Tyrosine-235 in the mobile loop region of domain I protein of transhydrogenase from *Rhodospirillum rubrum* strongly inhibit hydride transfer, *Biochim. Biophys. Acta 1320*, 265−274.
55. Gupta, S., Quirk, P. G., Venning, J. D., Slade, J., Bizouarn, T., Grimley, R. L., Cotton, N. P. J., and Jackson, J. B. (1998) Mutation of amino acide residues in the mobile loop region of the NAD(H)-binding redomain of proton-translocating transhydrogenase, *Biochim. Biophys. Acta 1409*, 25−38.
56. Johansson, C., Bergkvist, A., Fjellstrom, O., Rydstrom, J., and Karlsson, B. G. (1999) NMR characterisation of the NADP(H)-binding domain of *Escherichia coli* transhydrogenase: sequential assignment and global fold, *FEBS Lett. 458*, 180−184.
57. Johansson, C., Pedersen, A., Karlsson, B. G., and Rydstrom, J. (2002) Redox-sensitive loops D and E regulate NADP(H) binding in domain III and domain I-domain III interactions in proton-translocating *Escherichia coli* transhydrogenase, *Eur. J. Biochem. 269*, 4505−4515.
58. Jackson, J. B., Quirk, P. G., Cotton, N. P. J., Venning, J. D., Gupta, S., Bizouarn, T., Peake, S. J., and Thomas, C. M. (1998) Interdomain hydride transfer in proton-translocating transhydrogenase, *Biochim. Biophys. Acta 1365*, 79−86.
59. Fjellstrom, O., Bizouarn, T., Zhang, J., Rydstrom, J., Venning, J. D., and Jackson, J. B. (1999) Catalytic properties of hybrid complexes of the NAD(H)-binding and NADP(H)-binding domains of the proton-translocating transhydrogenases from *Escherichia coli* and *Rhodospirillum rubrum*, *Biochemistry 38*, 415−422.
60. Yamaguchi, M., and Stout, C. D. (2003) Essential glycine residues in the proton channel of *Escherichia coli* transhydrogenase, *J. Biol. Chem. 278*, 45333−45339.
61. Bragg, P. D., and Hou, C. (2001) Characterisation of mutants of beta-histidine91, beta-aspartate213 and beta-asparagine222, possible components of the energy-transduction pathway of the proton-translocating pyridine nucleotide transhydrogenase of *Escherichi coli*, *Arch. Biochem. Biophys. 388*, 299−307.
62. Karlsson, J., Althage, M., and Rydstrom, J. (2003) Roles of individual amino acid in helix 14 of the membrane domain of proton-translocating transhydrogensae from *Escherichia coli* as deduced from cysteine mutagenesis, *Biochemistry 42*, 6575−6581.
63. Weber, J., and Senior, A. E. (2003) ATP synthesis driven by proton transport in F_1F_o-ATP synthase, *FEBS Lett. 545*, 61−70.
64. Meuller, J., and Rydstrom, J. (1999) The membrane topology of proton-pumping *Escherichia coli* transhydrogenase determined by cysteine labeling, *J. Biol. Chem. 274*, 19072−19080.
65. Studley, W. K., Yamaguchi, M., Hatefi, Y., and Saier, M. H. (1999) Phylogenetic analyses of proton-translocating transhydrogenases, *Microb. Comp. Genomics 4*, 173−186.

BI0497594